Food Bioprocess Technol (2015) 8:916–925
DOI 10.1007/s11947-014-1460-1

ORIGINAL PAPER

Effects of Freezing Temperature and Water Activity on Microstructure, Color, and Protein Conformation of Freeze-Dried Bluefin Tuna (*Thunnus orientalis*)

Nathdanai Harnkarnsujarit · Kiyoshi Kawai · Toru Suzuki

Received: 10 September 2014 / Accepted: 9 December 2014 / Published online: 20 December 2014

Abstract Freeze-drying of muscle foods including bluefin tuna (*Thunnus orientalis*) effectively restricted microbial growth and prolonged shelf life; however, microstructures and protein conformation changes possibly take place which contribute to functional and quality loss. This study aimed to investigate the effects of freezing and water sorption on microstructure, color, and conformation changes of protein in freeze-dried tuna. Tuna were frozen at various freezing temperatures prior to freeze-drying and stored at different a_w at 25 °C. X-ray computed tomography revealed microstructures of freeze-dried solids and reflected ice formation in parallel to the muscle fiber. Higher temperature freezing gave a slower nucleation and subsequent larger ice crystals formed, which enhanced aggregation of muscle fiber resulting in a thicker size but less integrity of fibrous structures. Water sorption induced structural changes of solids stored at above T_g in concurrent with the acceleration of browning which attributed to the increased molecular mobility. Attenuated total reflectance Fourier transform infrared spectroscopy indicated that freeze-dried tuna undergoing all freezing temperatures revealed a significant frequency shift and broadening of amide I band mainly associated with stretching vibrations of the C=O bond as a_w increased. The increased intermolecular interaction via hydrogen bonding was found in high a_w systems. The results indicated that a faster freezing increased protein stability in freeze-dried tuna but accelerated browning induced by water sorption which increased molecular mobility of solids above T_g.

Keywords Freezing · Microstructure · Tuna · Browning · Protein · Water activity

N. Harnkarnsujarit
Department of Packaging and Materials Technology, Faculty of Agro-Industry, Kasetsart University, 50 Ngam Wong Wan Rd, Bangkok 10900, Thailand

N. Harnkarnsujarit (✉) · T. Suzuki
Department of Food Science and Technology, Tokyo University of Marine Science and Technology, 4-5-7, Konan, Minato-ku, Tokyo, Japan
e-mail: nathdanai.h@ku.ac.th

K. Kawai
Department of Biofunctional Science and Technology, Graduate School of Biosphere Science, Hiroshima University, 1-4-4 Kagamiyama, Higashi-Hiroshima, Hiroshima, Japan

Introduction

Pacific bluefin tuna (*Thunnus orientalis*) is high-value seafood widely caught in Japan. However, various deteriorations including chemical reactions, physical change, and growth of microorganisms immediately take place after harvesting, leading to a lower quality and shelf life of fish products (Zhu et al. 2013). Freezing and dehydration help prolong shelf life for storage and distribution of such fishery products.

Freeze-drying is a well-known dehydration process to preserve and maintain high quality of perishable products and it can be applied mostly to high-valued materials because of the high energy consumption and production cost. The limited microbial growth in freeze-dried products attributes to a low water activity and hence prolongs shelf life. The freeze-drying process consists of freezing and ice sublimation under reduced pressure. The freezing causes phase separation between pure ice and freeze-concentrated solutes in high-water food systems, and the pores are left embedded in the solids after the ice is sublimated (Roos 1997). The nucleation and crystal growth during freezing control microstructure formation of freeze-dried solids which subsequently impact chemical reaction and hence the stability of solid materials such as the Maillard reaction (White and Bell 1999), enzymatic browning (Acevedo et al. 2008), lipid oxidation (Nelson and Labuza 1992), and subsequent degradation of encapsulated

components (Harnkarnsujarit et al. 2012). The microstructure of freeze-dried materials has usually been analyzed by means of scanning electron microscopy (White and Bell 1999; Harnkarnsujarit et al. 2012); however, the monitoring is limited to two-dimensional and, therefore, other three-dimensional measurement technique such as X-ray computed tomography (X-ray CT) may potentially provide more details of the microstructure including different directions and layers in solid materials. This technique was recently applied to food and agricultural products, and no studies utilize X-ray CT to monitor fibrous structure in muscle food systems.

Glass transition determines stability of amorphous materials including dehydrated and freeze-dried foods. Water sorption increases molecular mobility exponentially above the glass transition temperature which results in rapid deterioration of dehydrated foods as well as their protein components in the solid state via chemical and physical modification (Lai and Topp 1999; Acevedo et al. 2006; Rahman et al. 2009; Roos 2009; Manning et al. 2010; Rao and Labuza 2012).

The infrared spectra of protein molecules can be correlated directly to the conformation of protein back bone (Payne and Veis 1988) and has been widely used to determine instability of protein materials undergoing processing and storage (Payne and Veis 1988; Griebenow and Klibanov 1995; Fu et al. 1999; Chu et al. 2001; Pikal et al. 2008). The exact frequency of the amide I and II absorptions would be predicted to be influenced by the strength of any hydrogen bonds involving amide C=O and N-H groups, respectively (Jackson and Mantsch 1991, 1995). The denaturation followed by aggregation of protein affects their functional properties such as hydration/solubility and textural properties (Zhou et al. 2008). The instability of protein in the solid state has been widely reported in model systems; however, the demonstrations of the conformational changes of protein in dehydrated foods including bluefin tuna during storage are rare. Understanding factors affecting protein stability in freeze-dried solids would improve processing and packaging conditions to retain protein quality in foods.

The objective of this study was to investigate the effects of freezing temperature and water activity on the microstructure and protein conformation of freeze-dried bluefin tuna. In the present study, the X-ray CT was also performed to visualize the integrity of muscle fiber in freeze-dried tuna. The rate of protein conformational change was derived from the kinetics equation. Moreover, the browning discoloration as affected by the freezing and water sorption was also demonstrated.

Materials and Methods

Freezing and Freeze-Drying of Tuna

Bluefin tuna (*T. orientalis*) was purchased from the seafood market in Tokyo, Japan. The tuna was sectioned, and the middle of back meat was frozen on the same day of distribution. The back meat was cut into approximately 2-cm cubes. The tuna cubes were placed on aluminum tray and prefrozen for 16 h at −20, −50, and −90 °C in chest freezers to obtain various cooling rates of tuna. The prefreezing temperatures were chosen according to the trial experiments to control various cooling rates and freezing time and hence ice formation in tuna as shown in Table 1. The frozen tuna samples were subsequently transferred to store at −90 °C for further 3 h to reduce ice temperature and prevent ice melting during transfer to freeze-dryer. The temperature of tuna during freezing was collected every 1 s with type-T thermocouples (copper–constantan) connected to a data logger (Memory HiLOGGER LR8431, HIOKI E.E. Corporation, Nagano, Japan). The frozen tuna samples were freeze-dried at below 100 Pa in a freeze-dryer (Kyowac, Kyowa Vacuum Engineering Co., Ltd., Tokyo, Japan) with step increase of shelf temperatures every 6 h for 5 °C from −40 to 5 °C and 10 °C from 5 to 25 °C. The vacuum was released with an ambient air. The freeze-dried tuna cubes were removed and stored in an evacuated desiccator containing P_2O_5 for 5 days to remove residual water prior to the measurement.

Water Sorption

Approximately 1 g of freeze-dried tuna prefrozen at −90 °C was transferred into glass vials and stored in evacuated desiccators at 25 °C, which contained various saturated salt solutions namely LiCl, CH_3COOK, $MgCl_2$, K_2CO_3, $MgNO_3$, Na_2NO_2, and NaCl (Wako Pure Chemical Co., Ltd., Osaka, Japan) and corresponding water activity (a_w) of 0.11, 0.22, 0.33, 0.44, 0.55, 0.66, and 0.75, respectively. Samples were removed from the desiccators and immediately closed with caps to prevent moisture transfer to the environment, and triplicate samples were weighed using a digital balance (±0.00001 g) at interval during storage.

The Guggenheim-Anderson-de Boer (GAB) model (Eq. 1) was fitted to the experimental steady state water contents (m) at 192 h of storage to determine the sorption isotherms of freeze-dried tuna and parameters m_m (monolayer value), K, and C constant were derived from regression analysis (Eq. 2).

$$m = \frac{m_m C K a_w}{(1-Ka_w)(1-Ka_w + CKa_w)} \quad (1)$$

Table 1 Freezing properties of tuna frozen at −20, −50, and −90 °C

Freezing properties	−20 °C	−50 °C	−90 °C
Cooling rate (°C/min)	0.3±0.1	0.8±0.2	1.8±0.5
Initial freezing temperature, T_i (°C)	−2.6±0.5	−4.7±1.1	−4.7±0.3
Freezing time (min)	194±28	53±13	15±9

Values shown are mean±SD from triplicate measurements

$$\frac{a_w}{m} = \alpha a_w^2 + \beta a_w + \gamma \quad (2)$$

where

$$K = \frac{\left(\sqrt{\beta^2 - 4\alpha\gamma}\right) - \beta}{2\gamma} \quad (3)$$

$$C = \left(\frac{\beta}{\gamma K}\right) + 2 \quad (4)$$

$$m_m = \frac{1}{\gamma K C} \quad (5)$$

Glass Transition Measurement

The water-soluble fraction of fresh tuna was extracted and freeze-dried to measure the glass transition temperature (T_g) using differential scanning calorimetry (DSC) and compared with the T_g values of whole tuna previously reported by Orlien et al. (2003). Deionized water (water distillation apparatus RFD 240RA, Advantec®, Toyo Seisakusho Kaisha Ltd., Osaka, Japan) was added to fresh tuna meat in a weight ratio of 2:1 and homogenized (AM-3 ACE Homogenizer, Nihonseiki Kaisha Ltd., Tokyo, Japan) at 10,000 rpm for 5 min in an ice water bath to prevent heat generation. The mixtures were subsequently centrifuged at 20,000 g for 10 min at 4 °C using a high-speed refrigerated centrifuge (Suprema 21, NA22 Rotor, TOMY Digital Biology Co., Ltd., Tokyo, Japan), and the supernatant was collected and freeze-dried as previously described. The freeze-dried tuna fraction was stored in evacuated desiccator containing P_2O_5 to remove residual water for 5 days prior to the measurement.

Approximately 10–15 mg of freeze-dried water-soluble fraction was transferred to aluminum DSC pans and stored in desiccators which contained saturated salt solutions of $MgCl_2$, $MgNO_3$, and NaCl and given a_w values of 0.33, 0.55, and 0.75, respectively. Duplicate samples were measured for the T_g using a PYRIS Diamond™ DSC (Perkin Elmer, Connecticut, USA) connected to a cryofill liquid nitrogen cooling system (Perkin Elmer). Duplicate samples were measured within the range of −80 to 80 °C at a rate of 5 and 10 °C/min for the heating and cooling scan, respectively. The experimental T_g value was derived from the onset temperature of the second scan using a PYRIS software for Windows (version 7.0.0.0110, Perkin Elmer). The T_g of anhydrous and a_w 0.11 samples was measured using a micro-DSC VII Evo (SETARAM, KEP Instrumentation, Caluire, France). The freeze-dried tuna fraction was stored in evacuated desiccators containing P_2O_5 and LiCl contributed to anhydrous and a_w 0.11 samples, respectively. Approximately 130 mg of samples was transferred into a standard hastelloy DSC cell and scanned from −10 to 80 °C at a rate of 1 °C/min in duplicate. The T_g was derived from the onset temperature of a second scan using the Calisto software (version 1.14, SETARAM, KEP Instrumentation). The empty cell was used as the reference for the DSC measurement.

X-ray Microtomography

The freeze-dried tuna cubes were measured for the microstructures using the Skyscan 1172 X-ray microcomputed tomography system (X-ray CT, Bruker, Kontich, Belgium). The freeze-dried tuna was wrapped with a cling film to prevent water adsorption and mounted on a rotational plate. The X-ray voltage and current was 54 kV and 100 μA, respectively. A CCD camera with 2,000×1,332 pixels was used to record the transmission of the conical X-ray beam through all samples. The distance source-object-camera was adjusted to produce images with a pixel size of 13.59 μm. Two frames averaging a rotation step of 0.4° with 10 random movement and an exposure time of 1,840 ms were chosen covering a view of 180° contributed to the scan time of 60 min. Three-dimensional reconstruction of samples was created by stacking of two-dimensional tomographs from a total of 800–1,000 slices with a slice spacing of 0.013 mm using the reconstruction NRecon software (version 1.6.8.0, Bruker). A ring artifact reduction (set to 7) and beam hardening correction (52 %) were performed with NRecon software.

The reconstructed images were processed and analyzed for the pore size, surface area, and solid wall thickness using a Skyscan CTAn software (CT-Analyzer version 1.12.10.0, Bruker). The images were first converted to a binary image of black and white color and the gray-scale thresholds were adjusted to match the solid and void spaces of the raw images.

Attenuated Total Reflectance Fourier Transforms Infrared Microscopy

The freeze-dried tuna was cut into approximately 12×6 mm with 2-mm thickness and stored at different a_w conditions as previously described. The samples were removed from the desiccators at 25 °C for the attenuated total reflectance Fourier transforms infrared microscopy (ATR-FTIR) measurement at intervals during storage for 31 days.

The infrared absorbance was measured using an ATR-FTIR (Nicolet iN10 MX, Thermo Fisher Scientific, Wisconsin, USA) equipped with a Germanium crystal (ATR crystal). The specimens were placed on a microscopic glass slide and placed on the FTIR stage. A reference background absorbance spectrum was taken from the ambient air with a clean empty crystal. The spectra were recorded from 128 co-

added scans in a wave number range of 4,000–800 cm^{-1} at a resolution of 4 cm^{-1} at 25 °C. Spectra from different points in freeze-dried tuna were collected for each sample and averaged (three to five replicates) using the OMNIC Picta software (version 1.0, Thermo Fisher Scientific). The collected spectrum was ratioed against the reference background spectrum to obtain the spectrum of a freeze-dried tuna.

The baseline-corrected spectra were analyzed for the second derivative of amide I band for initial monitoring of number of components and peak positions. Fourier self-deconvolution of amide I band was performed using an OMNIC 8.2 software (Thermo Fisher Scientific) at a bandwidth of 30 cm^{-1} and an enhancement factor of 3.

The rate constants for protein conformation changes during storage were derived from the first-order kinetics: $-kt=\ln A/A_0$. Accordingly, the frequency shift of amide I maximum at storage intervals divided by the initial frequency (A/A_0) was converted to a natural logarithmic form (ln), and the rate constants (k) were derived from the slope of linear regression ($R^2 \geq 0.84$).

Statistical Analysis

Data were subjected to analysis of variance (ANOVA), and mean comparison were carried out using Duncan's multiple range test at 95 % confidence intervals. Moreover, the significant differences of first-order rate constants ($P \leq 0.05$) for FTIR band shifts were determined among linear regressions by analysis of covariance (ANCOVA). Statistical analysis was performed using a SPSS 17.0 software for Windows (SPSS Inc., Chicago, USA).

Results and Discussion

Freezing and Microstructure of Freeze-Dried Tuna

The temperature of tuna cube frozen at −20, −50, and −90 °C and their freezing properties as derived from the freezing curve are shown in Fig. 1 and Table 1, respectively. The cooling rates were derived from the initial slope of the freezing profile. The results confirmed that a lower temperature freezing gave a faster cooling rate and a shorter freezing time. The tuna frozen at −50 and −90 °C had a similar initial freezing point (T_i) whereas the freezing at −20 °C led to a significantly higher T_i ($P \leq 0.05$). The decreased freezer temperature from −20 to −50 °C and −90 °C resulted in a significant ($P \leq 0.05$) reduction of freezing time for 73 and 92 %, respectively. A decreased freezing time contributes to shorter time which allows for the ice growth. Accordingly, the low temperature freezing gave a fast cooling rate which enhanced nucleation,

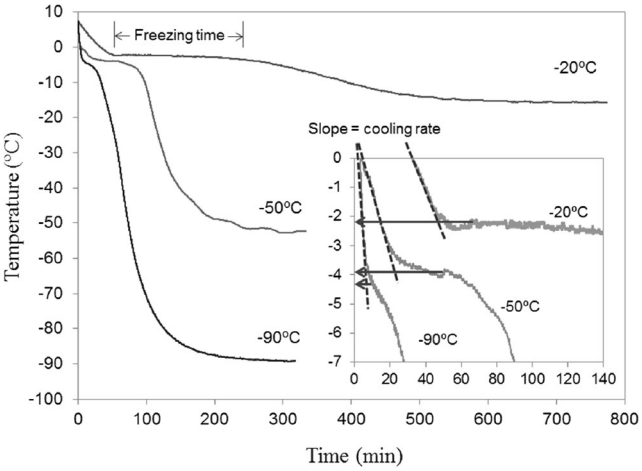

Fig. 1 Freezing curve of fresh tuna frozen at −20, −50, and −90 °C. *Inlet* figure shows the first 140 min of freezing. The *dotted lines* and *arrows* indicate initial slope and initial freezing temperature (T_i), respectively. Freezing time refers to the period in which liquid water transform into ice

and limited time of the ice growth contributed to a high number of small ice crystals formed during freezing.

The X-ray CT demonstrated three dimensions of solid microstructures and, therefore, allowed for monitoring the material structures in different direction. Figure 2 shows the X-ray CT images of freeze-dried tuna prefrozen at −20, −50, and −90 °C in parallel and cross section to muscle fiber. The results indicated that the ice formed in parallel to the direction of protein fibers in which the size depended on the freezing conditions. The connectivity of fibrous structures suggests integrity of the muscle fiber as a result of freezing. The systems prefrozen at −20 °C had the thickest size (33± 1 μm) but least integrity of fibrous structures compared to the systems prefrozen at −50 and −90 °C. The larger size of ice crystals formed during freezing at −20 °C caused a high disruption of fibrous structure as revealed by the least connectivity of muscle fiber. Moreover, high disconnectivity of muscle fibers suggested a higher open pore in three dimensions of freeze-dried tuna which possibly affect the transportation of gas such as oxygen and subsequent oxidative reaction as discussed later. Moreover, freezing causes phase separation between water and solutes and accelerated aggregation of muscle fiber as indicated by the thickness of the solid membrane surrounding the pores (Fig. 2d–f). Large sizes of ice crystals enhanced protein fiber aggregation and hence thicker sizes of membrane solids were formed in higher temperature freezing.

Glass Transition Temperature and Water Sorption

The glass transition temperature (T_g) of freeze-dried water-soluble fraction (WSF), whole muscle (WM) tuna, and water sorption isotherm of freeze-dried tuna at various water activities (a_w) are shown in Fig. 3. As expected, WSF had lower T_g

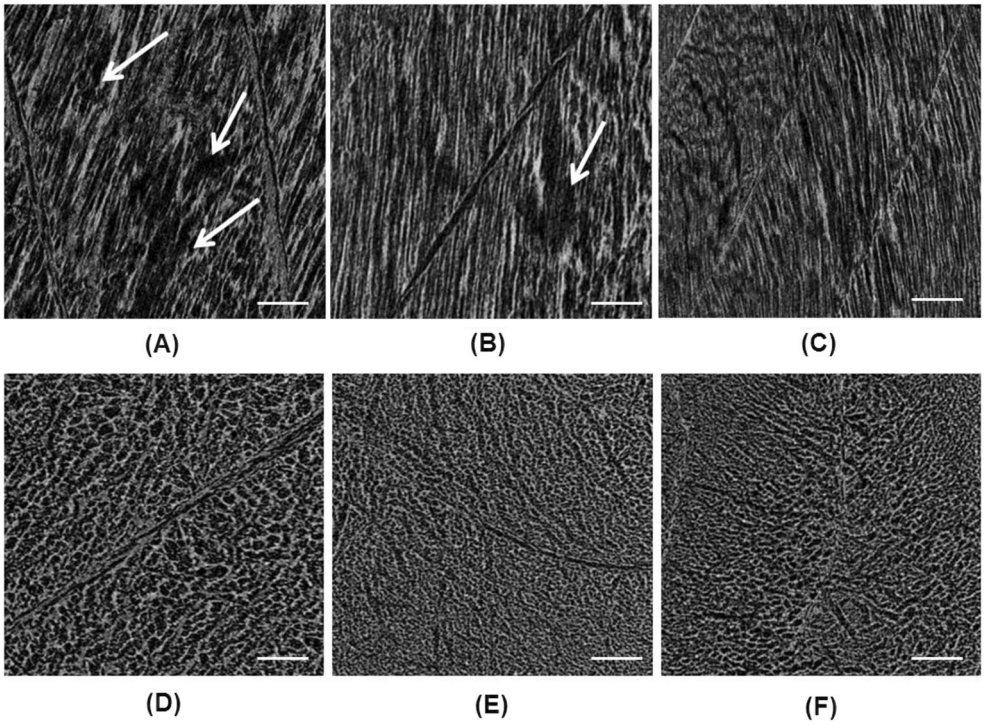

Fig. 2 X-ray CT images of freeze-dried tuna prefrozen at −20 °C (**a**, **d**), −50 °C (**b**, **e**), and −90 °C (**c**, **f**) prior to freeze-drying showing the microstructures in parallel (**a**, **b**, **c**) and cross section (**d**, **e**, **f**) to muscle fiber (*scale bar*=1 mm). *Arrows* indicate the disconnectivity of the muscle fiber. *Dark color* reflects void space embedded in solid phase of muscle structure

values than WM reported by Orlien et al. (2003). The WSF of fresh tuna consists of low-molecular-weight salt, sugars, and water-soluble sarcoplasmic proteins including myoglobin, hemoglobin, globins, albumins, and some enzymes (Orlien et al. 2003; Tahergorabi et al. 2011) which act as plasticizers which contributed to a slightly lower T_g value. T_g of dehydrated food solids is strongly influenced by hydrophilic components (Roos 2009). The smaller molecular weight solutes act as plasticizers of larger molecular weight solutes which decrease T_g depending on ratio of solute composition. Accordingly, WM contained a high amount of large-molecular-weight solutes particularly protein components leading to a higher T_g values. Hashimoto et al. (2004) also revealed a plasticization effect of low-molecular-weight materials in WM tuna as less T_g values were found than those of extracted muscle proteins (sarcoplasmic and myofibrillar proteins). It should be emphasized that the T_g values of WSF revealed the maximum plasticization effect of low-molecular-weight solute components in tuna muscle, and thus clearly confirmed that the anhydrous and a_w 0.11 systems were in the glassy state. The difference between T_g values of WSF and WM decreased with increased a_w as water is a strong plasticizer of dehydrated food solids and confirmed a strong influence of hydrophilic phase on solid T_g.

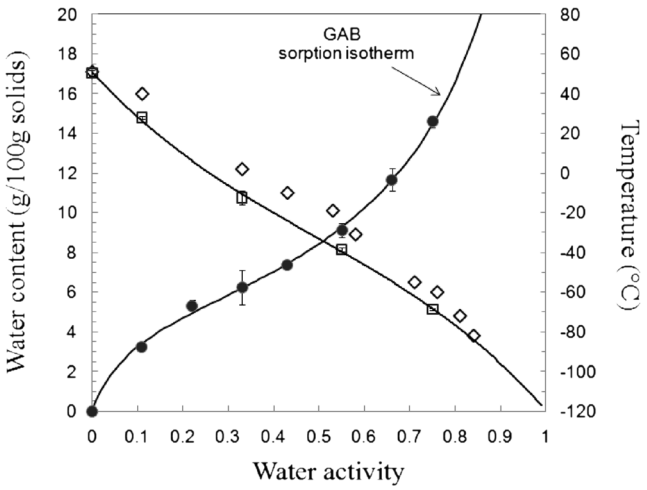

Fig. 3 Water sorption of freeze-dried whole muscle tuna (WM) and glass transition temperatures (T_g) of freeze-dried water-soluble fraction (WSF) tuna stored at various water activities (a_w) at 25 °C. *Error bars* indicate standard deviation derived from N=3 and N=2 for experimental WM water sorption and WSF T_g, respectively. *Circles* and *square symbols* represent experimental water content and T_g, respectively. The reference T_g values of freeze-dried WM tuna reported by Orlien et al. (2003) are given as the *diamond symbols* (with permission from Orlien et al. (2003) The question of high- or low-temperature glass transition in frozen fish. Construction of the supplemented state diagram for tuna muscle by differential scanning calorimetry. Journal of Agricultural and Food Chemistry, 51 (1), 211–217. Copyright 2003 American Chemical Society)

The increased a_w led to a decreased T_g of freeze-dried solids which confirmed the plasticization effect of water. Both the physical state of amorphous food solids and stability are extremely sensitive to water at low water contents; therefore, modeling and prediction of water sorption properties are particularly important in predicting shelf life of low- and intermediate-water food systems (Roos 2009). The GAB water sorption calculation of the experimental data reveals that the monolayer water content (m_m) of freeze-dried tuna is 5.21 g/100 g solids from the derived C and K constant of

13.77 and 0.87, respectively. The freeze-dried tuna shows a sigmoidal curve which represents type II isotherm (Fig. 3).

Water Sorption and Quality Changes of Freeze-Dried Tuna

Microstructure

Water is a strong plasticizer increasing free volume of solids. The increased water sorption plasticized and decreased T_g of solids contribute to the decrease of solid viscosity and relaxation time (Roos 2009). Consequently, structural changes of dehydrated materials take place above T_g. The image analysis of X-ray CT revealed the solid and void properties of freeze-dried tuna stored at various a_w for 31 days (Table 2). A higher temperature freezing led to a larger pore diameter, higher surface area, and larger thickness as previously discussed. The water sorption showed an insignificant effect ($P>0.05$) on the changes of surface area and pore diameter of freeze-dried tuna prefrozen at −20 °C which was possibly caused by a high disconnectivity of the muscle solids as damaged by the large ice crystals and hence limited the accuracy of void measurement. However, the increased a_w led to a decreased size of surface area and pore diameter in systems prefrozen at −50 and −90 °C which had a higher connectivity of the solid membrane surrounded pores. Moreover, the water sorption slightly increased the membrane thickness of freeze-dried tuna prefrozen at −90 °C. The gradual sorption of water by the dry matrix caused swelling of biopolymer, i.e., protein (Das and Das 2002) and, therefore, increased the thickness of solids but reduced the size of surface area and pore diameter.

Discoloration

Figure 4 shows the appearance of freeze-dried tuna prefrozen at −20 and −90 °C after storage at various a_w for 7 days. Browning was clearly evident at and above a_w 0.33 which corresponded to the storage conditions above T_g of solids (Fig. 3). The brown pigmentation in freeze-dried muscle food and high-protein systems have been reported to be caused by non-enzymatic Maillard reaction which was accelerated at intermediate and high a_w (Aguilera et al. 1993; White and Bell 1999; Acevedo et al. 2006; Shah et al. 2009). Although tuna contains a small amount of carbohydrate including reducing sugars, the formation of secondary lipid oxidation products such as aldehyde and other carbonyl compounds during storage can participate in Maillard reaction with amino acid compounds, resulting in browning (Zamora and Hidalgo 2005; Shah et al. 2009; Rao and Labuza 2012). In addition, the autoxidation of myoglobin to metmyoglobin (George and Stratmann 1952) possibly caused a dark pigmentation and therefore, increased the brown discoloration in freeze-dried tuna.

Table 2 Pore diameter, surface area, and solid wall thickness of freeze-dried tuna prefrozen at −20, −50, and −90 °C prior to freeze-drying and subsequently stored at anhydrous and various a_w conditions at 25 °C for 31 days as determined by X-ray CT image analysis

Microstructure properties	Anhydrous			a_w 0.22			a_w 0.55			a_w 0.75		
	−20 °C	−50 °C	−90 °C	−20 °C	−50 °C	−90 °C	−20 °C	−50 °C	−90 °C	−20 °C	−50 °C	−90 °C
Pore diameter range (max–min, μm)	150–80	137–73	118–62	158–84	141–73	116–58	141–80	134–65	121–58	150–81	116–63	117–57
Average pore diameter (μm)	92 ± 3^{ab}	84 ± 6^{bc}	73 ± 2^{de}	97 ± 1^{a}	86 ± 10^{bc}	71 ± 1^{ef}	92 ± 7^{ab}	80 ± 7^{cd}	74 ± 1^{de}	94 ± 2^{ab}	75 ± 2^{de}	71 ± 2^{ef}
Surface area (μm)	540 ± 24^{a}	489 ± 41^{ab}	408 ± 23^{c}	574 ± 13^{a}	475 ± 87^{bc}	372 ± 11^{cd}	470 ± 38^{bc}	419 ± 43^{c}	348 ± 4^{d}	511 ± 22^{ab}	358 ± 20^{cd}	352 ± 28^{d}
Average thickness (μm)	33 ± 1^{b}	31 ± 2^{bc}	27 ± 1^{d}	37 ± 1^{a}	32 ± 3^{b}	27 ± 0^{d}	36 ± 3^{a}	30 ± 2^{bc}	30 ± 0^{bc}	36 ± 1^{a}	30 ± 1^{bc}	28 ± 0^{cd}

The different superscript letters indicate the significant difference ($P\leq0.05$) within the same row Values shown are mean±SD from triplicate measurements

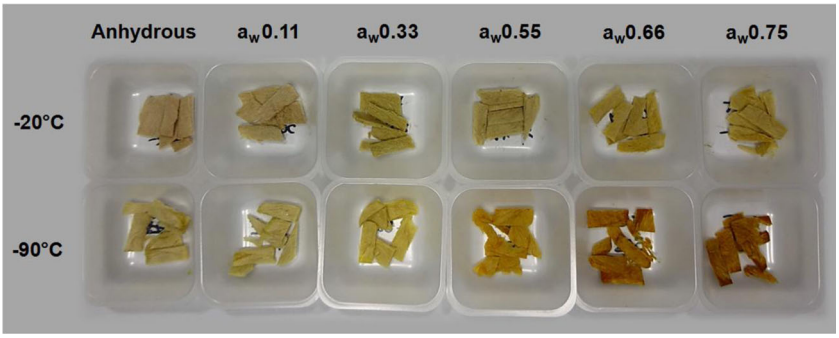

Fig. 4 Appearance of freeze-dried tuna prefrozen at −20 and −90 °C prior to freeze-drying and stored at various water activities (a_w) at 25 °C for 7 days showing the browning development as a function of a_w. For color visualization, the readers are encouraged to access the online version of the manuscript

The results also indicated a higher browning intensity in freeze-dried tuna prefrozen at −90 °C than the system prefrozen at −20 °C which presumed to cause by the difference of matrix microstructure and subsequent oxygen accessibility to accelerate oxidation. Previous study suggested that the thickness of solid membrane surrounding the pores affects the oxygen permeability through solids and hence increased oxidative degradation of encapsulated component, i.e., β-carotene (Harnkarnsujarit et al. 2012). Systems prefrozen at −20 °C stored at anhydrous and a_w 0.11 corresponded to below T_g remained a higher intense oxymyoglobin as reflected by the pink color. Conversely, the systems prefrozen at −90 °C show a slightly yellowish color which was possibly caused by the accelerated oxidation taking place in the glassy state and a subsequent transformation of myoglobin that confirmed a higher degree of oxidation. The results reflected a higher degree of oxidation in systems prefrozen at −90 °C than systems prefrozen at −20 °C because (1) a high number of smaller pore sizes in solids led to a higher surface area to oxygen exposure and (2) a thinner size of muscle fiber possibly enhanced oxygen penetration through solids and increased oxidation. Although tuna prefrozen at −20 °C had a higher open pore as a result of muscle fiber disintegrity which possibly led to high oxygen transportation, the dense and thicker size of muscle fiber possibly limited the oxygen exposure to cause oxidative reaction. The results suggest that the surface area was a major factor affecting oxidation in freeze-dried tuna.

The increased water sorption up to a_w 0.75 accelerated browning development in agreement with the studies of Saltmarch and Labuza (1982) and Acevedo et al. (2006) who showed the maximum of Maillard browning as a_w increased up to a_w 0.7–0.8 depending on solid food materials. Rahman et al. (2009) also reported an increase of peroxide value suggesting the lipid oxidation in freeze-dried grouper as the increased water sorption (from 5 to 20 g/100 g solids). The water plasticization increased molecular mobility as a function of T-T_g which accelerated various physicochemical changes including browning reaction and lipid oxidation in high-protein systems (White and Bell 1999; Acevedo et al. 2006; Rahman et al. 2009; Rao and Labuza 2012).

Protein Conformation

The instability of protein affects their functional properties such as hydration/solubility and textural properties of dehydrated high-protein foods (Zhou et al. 2008). The FTIR spectra reveal the secondary structures of protein in freeze-dried tuna which was mostly reflected by major amide I and amide II bands (Fig. 5). The amide I band was observed within a range of 1,600–1,700 cm^{-1} which involves mainly to stretching vibration of νC=O along the polypeptide backbone (Byler and Susi 1986; Payne and Veis 1988; Jackson and Mantsch 1991). The amide II band located between 1,480 and 1,580 cm^{-1} and represents δN-H bending (60 %) and νC-N stretching (40 %) vibrations (Jackson and Mantsch 1995; Pelton and McLean 2000). The infrared spectra of amide I and II region of proteins are very sensitive to their secondary structures (Dousseau and Pezolet 1990). Most researchers have found that amide I absorption is more useful for determination of protein secondary structures than amide II, probably due to the fact that it effectively arises primarily

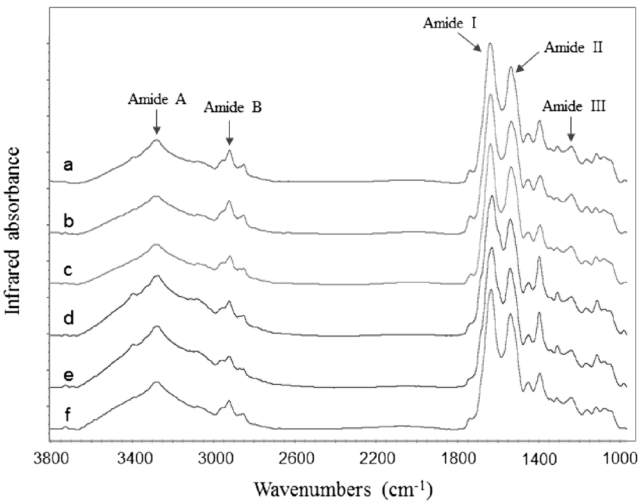

Fig. 5 ATR-FTIR spectra of freeze-dried tuna underwent various prefreezing (−20, −50, and −90 °C) prior to freeze-drying and stored at different a_w (0.55 and 0.75) conditions at 25 °C for 31 days: **a** −20 °C and a_w 0.55, **b** −50 °C and a_w 0.55, **c** −90 °C and a_w 0.55, **d** −20 °C and a_w 0.75, **e** −50 °C and a_w 0.75, and **f** −90 °C and a_w 0.75

from only one of the amide functional groups, in contrast to the amide II mode (Jackson and Mantsch 1995). The results also showed only a slight frequency shift of amide II (approximately 5 cm^{-1}) during storage and, therefore, the amide I adsorption and their secondary components was investigated.

Figure 6 demonstrates the IR frequency shift in freeze-dried tuna prefozen at various freezing temperatures for amide I during storage up to 31 days at a_w 0.55 and 0.75 conditions. The conformation changes of proteins were suggested by the shift of amide I bands which indicate secondary structures of proteins (Byler and Susi 1986; Jackson and Mantsch 1991, 1995; Fu et al. 1999; Pelton and McLean 2000). The amide I band showed a shift to lower wave numbers of 10–20 cm^{-1} (Fig. 6) during storage at high a_w of 0.55 and 0.75 which suggested an increased strength of hydrogen bonding (Torii et al. 1998; Barth 2007). It is well established that the stronger the hydrogen bond involving the amide C=O, the lower the electron density and lengthen the C=O double bond. Consequently, the energy required to displace the oxygen atom from the carbon is reduced. Therefore, a lower photon energy is required which contributes to an absorption peak at a lower frequency of the amide I in the IR spectrum of protein (Payne and Veis 1988; Jackson and Mantsch 1991, 1995). Payne and Veis (1988) reported the frequency shift of IR spectra to lower wave numbers (up to 30 cm^{-1}) upon denaturation of gelatin and collagen. Accordingly, the present results suggested the denaturation which caused extended polypeptide chains and diminishes intramolecular hydrogen bonding. However, the extended nature of the polypeptides allows very close alignment of neighboring chains, which favors the formation of extremely strong intermolecular hydrogen bonds resulting in a corresponding low amide I maximum (Jackson and Mantsch 1995).

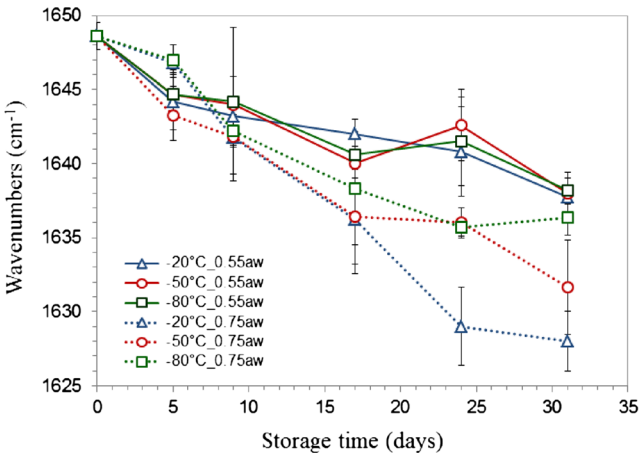

Fig. 6 Frequency shift of FTIR-amide I maximum in freeze-dried tuna prefrozen at −20 °C (*white triangle*), −50 °C (*white circle*), and −90 °C (*white square*) prior to freeze-drying and stored at a_w 0.55 (*full line*) and 0.75 (*dotted line*) at 25 °C for 31 days. Error bars indicate standard deviation calculated from three to four replicate samples

The experimental data for the frequency shift of amide I maximum during storage were fitted to zeroth-, first-, and second-order equations, and the highest correlation coefficients (R^2) was found for first-order kinetics (data not shown); therefore, the first-order rate constants for frequency shift of amide I maximum are shown in Table 3. The results indicated that the freezing conditions showed a significant effect on the rate of frequency shift at a high a_w of 0.75. Tuna prefrozen at −20 °C had the highest rate constants which indicated the fastest changes of protein secondary structures. Moreover, the systems prefozen at −20 °C showed the highest shift of amide I band after storage for 31 days at both a_w 0.55 and 0.75 conditions (10 and 20 cm^{-1}, respectively); whereas, the −90 °C systems showed the least frequency shift (Fig. 6). The freezing at −20 °C formed a thicker size of fibrous structure (Fig. 2) that contributed to a closer proximity of muscle fiber, which subsequently accelerated protein aggregation resulting in the fastest and highest conformation changes. While, tuna prefrozen at −90 °C had a slightly lower rate constant than −50 °C in concurrent with a slightly lower thickness of solid structure (Table 2). The results suggest the increased effect of microstructure on protein conformation changes as increased a_w and hence molecular mobility increased.

Freeze-dried tuna stored at anhydrous condition showed insignificant changes of protein conformation during storage up to 31 days (data not shown) which corresponded to the glassy state of solids. Conversely, the increased a_w led to the plasticization and accelerated the frequency shift of amide I band in concurrent with broadening of the band as increased a_w (Fig. 7a). Pikal et al. (2008) also found a denaturation in the solid state of freeze-dried model human growth hormone stored above glass transition of the system. The increased moisture enhances the hydrogen bond disruption associated with the helix-coil transition (protein unfolding); however, the glassy state, being more rigid with less molecular mobility, effectively prevents protein unfolding (Lai and Topp 1999; D'Cruz and Bell 2005). Costantino et al. (1994) demonstrated that water induced both covalent and non-covalent aggregation in lyophilized insulin in which the extent of aggregation directly correlated with the water uptake by the lyophilized

Table 3 First-order rate constants ($\times 10^{-4}$ day^{-1}) of the frequency shifts of amide I maximum in freeze-dried tuna prefrozen at −20, −50, and −90 °C and stored at a_w 0.55 and 0.75 at 25 °C for 31 days

Freeze-dried systems	−20 °C	−50 °C	−90 °C
a_w 0.55	2.58 (0.96) ^{aA}	2.42 (0.84) ^{aA}	2.47 (0.92) ^{aA}
a_w 0.75	6.10 (0.93) ^{aB}	4.23 (0.96) ^{abB}	3.64 (0.87) ^{bA}

Values in the parenthesis indicate correlation coefficient (R^2) of the experimental data fitting to a first-order kinetics calculation. The different superscript letters of the upper and lower case indicate the significant difference ($P \leq 0.05$) within the same column and row, respectively

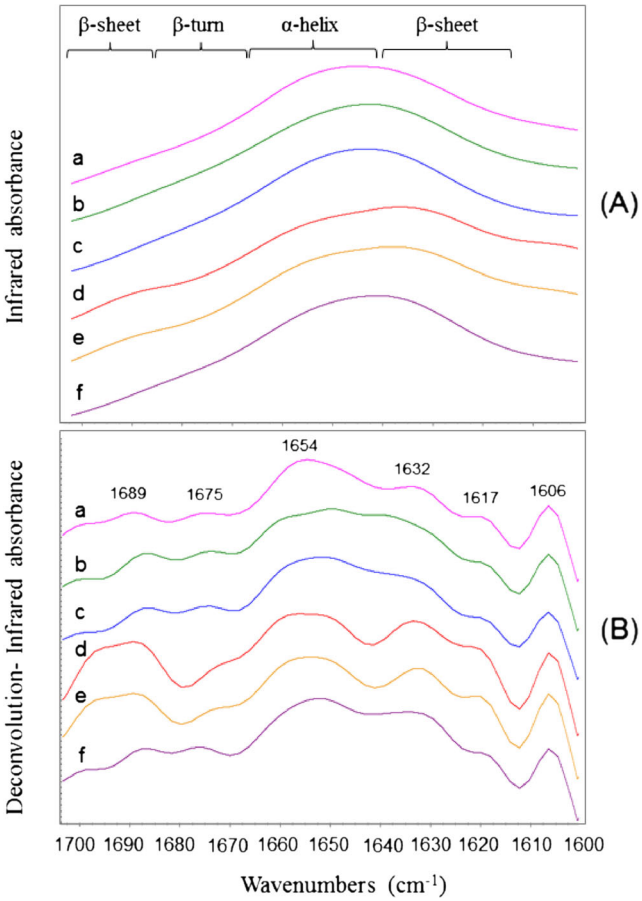

Fig. 7 FTIR-amide I bands (1,600–1,700 cm^{-1}) (**a**) and their deconvolution (**b**) of freeze-dried tuna underwent various prefreezing (−20, −50, and −90 °C) prior to freeze-drying and stored at different a_w (0.55 and 0.75) conditions at 25 °C for 31 days: **a** −20 °C and a_w 0.55, **b** −50 °C and a_w 0.55, **c** −90 °C and a_w 0.55, **d** −20 °C and a_w 0.75, **e** −50 °C and a_w 0.75, and **f** −90 °C and a_w 0.75

insulin powder, thus pointing to the critical role of protein conformational mobility in the aggregation process. The results clearly showed that the limited molecular mobility in the glassy state effectively stabilized protein structures; whereas, the water plasticization increased molecular mobility of solids and accelerated protein denaturation in freeze-dried tuna. The observed frequency shift in the present study is exclusively to be assigned to protein denaturation and interfering phenomena, e.g., non-enzymatic protein browning, myoglobin oxidation, and unsaturated fat oxidation can be ruled out.

Figure 7b shows the deconvolution of amide I bands between 1,600 and 1,700 cm^{-1} which consisted of six major components as determined by the second derivatives. The bands around 1,606, 1,654, and 1,675 were assigned to amino acid side chains, α-helix, and β-turn, respectively, while the β-sheet structure was reported to show several bands around 1,620, 1,634, and 1,690 (Fu et al. 1999; Chu et al. 2001). The major band of α-helix structure centered around 1,654 cm^{-1} had less intensity in higher a_w systems. The strong intense band around 1,690 cm^{-1} was observed in −20 and −50 °C systems stored at a_w 0.75 which suggested the increased proportion of β-sheet structure. The increase of β-sheet content, particularly in systems prefrozen at −20 and −50 °C, suggested an increased protein-protein interactions leading to the formation of intermolecular β-sheet structures (Griebenow and Klibanov 1995). The lowest β-sheet content in −90 °C systems stored at a_w 0.75 was in agreement with the slowest rate and least frequency shift of amide I band. The protein conformation changes as a conversion of α-helix and unordered to β-sheet structures has been reported in aggregated protein in the solid state (Griebenow and Klibanov 1995; Fu et al. 1999) as well as the denaturation of protein in hake during long-term frozen storage (Careche et al. 1999). The deconvolution of amide I band strongly support the influence of freezing and hence freeze-dried matrix structures on changes of protein conformation in high a_w systems.

Conclusion

The X-ray CT revealed that a higher temperature freezing formed a larger size of ice crystals and contributed to the least connectivity of protein fibrous structures. Conversely, the thinner size but higher integrity of fibrous structures formed in the low temperature freezing systems accelerated the browning discoloration in freeze-dried tuna. The results clearly state the effect of freezing on browning development in freeze-dried solids during storage. Water sorption plasticized and decreased the T_g of solids which accelerated browning and changes of protein conformation by the increased molecular mobility above T_g. ATR-FTIR showed the frequency shift of amide I bands indicating the changes of protein secondary structures of freeze-dried tuna. The higher a_w led to lower α-helix contents in concurrent with the increase of β-sheet structure as a result of the increased intermolecular interaction via hydrogen bonding. Moreover, high temperature freezing accelerated the conformation changes of protein in high a_w systems. The results suggest that the developments of freezing process and a_w are significant factors improving quality of freeze-dried high-protein and muscle foods including microstructure, color, and protein stability.

Acknowledgments The authors gratefully acknowledge the Ministry of Education, Culture, Sports, Science and Technology of Japan on the project title of "MEXT Revitalization Project for the Creation of Fisheries Research and Education Center in Sanriku" for the financial support.

References

Acevedo, N. C., Schebor, C., & Buera, M. P. (2006). Water–solids interactions, matrix structural properties and the rate of non-enzymatic browning. *Journal of Food Engineering, 77*(4), 1108–1115.

Acevedo, N. C., Briones, V., Buera, P., & Aguilera, J. M. (2008). Microstructure affects the rate of chemical, physical and color changes during storage of dried apple discs. *Journal of Food Engineering, 85*(2), 222–231.

Aguilera, J. M., Levi, G., & Karel, M. (1993). Effect of water content on the glass transition and caking of fish protein hydrolyzates. *Biotechnology Progress, 9*(6), 651–654.

Barth, A. (2007). Infrared spectroscopy of proteins. *Biochimica et Biophysica Acta (BBA)-Bioenergetics, 1767*(9), 1073–1101.

Byler, D. M., & Susi, H. (1986). Examination of the secondary structure of proteins by deconvolved FTIR spectra. *Biopolymers, 25*(3), 469–487.

Careche, M., Herrero, A. M., Rodriguez-Casado, A., Del Mazo, L., & Carmona, P. (1999). Structural changes of hake (Merluccius merluccius L.) fillets: effects of freezing and frozen storage. *Journal of Agricultural and Food Chemistry, 47*(3), 952–959.

Chu, H. L., Liu, T. Y., & Lin, S. Y. (2001). Effect of cyanide concentrations on the secondary structures of protein in the crude homogenates of the fish gill tissue. *Aquatic Toxicology, 55*(3), 171–176.

Costantino, H. R., Langer, R., & Klibanov, A. M. (1994). Moisture-induced aggregation of lyophilized insulin. *Pharmaceutical Research, 11*(1), 21–29.

D'Cruz, N. M., & Bell, L. N. (2005). Thermal unfolding of gelatin in solids as affected by the glass transition. *Journal of Food Science, 70*(2), E64–E68.

Das, M., & Das, S. K. (2002). Analysis of moisture sorption characteristics of fish protein myosin. *International Journal of Food Science and Technology, 37*(2), 223–227.

Dousseau, F., & Pezolet, M. (1990). Determination of the secondary structure content of proteins in aqueous solutions from their amide I and amide II infrared bands. Comparison between classical and partial least-squares methods. *Biochemistry, 29*(37), 8771–8779.

Fu, K., Griebenow, K., Hsieh, L., Klibanov, A. M., & Langera, R. (1999). FTIR characterization of the secondary structure of proteins encapsulated within PLGA microspheres. *Journal of Controlled Release, 58*(3), 357–366.

George, P., & Stratmann, C. J. (1952). The oxidation of myoglobin to metmyoglobin by oxygen. 1. *Biochemical Journal, 51*(1), 103.

Griebenow, K., & Klibanov, A. M. (1995). Lyophilization-induced reversible changes in the secondary structure of proteins. *Proceedings of the National Academy of Sciences, 92*(24), 10969–10976.

Harnkarnsujarit, N., Charoenrein, S., & Roos, Y. H. (2012). Porosity and water activity effects on stability of crystalline β-carotene in freeze-dried solids. *Journal of Food Science, 77*(11), 313–320.

Hashimoto, T., Suzuki, T., Hagiwara, T., & Takai, R. (2004). Study on the glass transition for several processed fish muscles and its protein fractions using differential scanning calorimetry. *Fisheries Science, 70*(6), 1144–1152.

Jackson, M., & Mantsch, H. H. (1991). Protein secondary structure from FT-IR spectroscopy: correlation with dihedral angles from three-dimensional Ramachandran plots. *Canadian Journal of Chemistry, 69*(11), 1639–1642.

Jackson, M., & Mantsch, H. H. (1995). The use and misuse of FTIR spectroscopy in the determination of protein structure. *Critical Reviews in Biochemistry and Molecular Biology, 30*(2), 95–120.

Lai, M. C., & Topp, E. M. (1999). Solid-state chemical stability of proteins and peptides. *Journal of Pharmaceutical Sciences, 88*(5), 489–500.

Manning, M. C., Chou, D. K., Murphy, B. M., Payne, R. W., & Katayama, D. S. (2010). Stability of protein pharmaceuticals: an update. *Pharmaceutical Research, 27*(4), 544–575.

Nelson, K A., & Labuza, T P. (1992). Relationship between water and lipid oxidation rates. In: Lipid oxidation in food (ACS Symposium Series 500), ed. St. Angelo AJ, American Chemical Society, Washington DC, pp 93–103.

Orlien, V., Risbo, J., Andersen, M. L., & Skibsted, L. H. (2003). The question of high-or low-temperature glass transition in frozen fish. Construction of the supplemented state diagram for tuna muscle by differential scanning calorimetry. *Journal of Agricultural and Food Chemistry, 51*(1), 211–217.

Payne, K. J., & Veis, A. (1988). Fourier transform IR spectroscopy of collagen and gelatin solutions: deconvolution of the amide I band for conformational studies. *Biopolymers, 27*(11), 1749–1760.

Pelton, J. T., & McLean, L. R. (2000). Spectroscopic methods for analysis of protein secondary structure. *Analytical Biochemistry, 277*(2), 167–176.

Pikal, M. J., Rigsbee, D., & Roy, M. L. (2008). Solid state stability of proteins III: calorimetric (DSC) and spectroscopic (FTIR) characterization of thermal denaturation in freeze dried human growth hormone (hGH). *Journal of Pharmaceutical Sciences, 97*(12), 5122–5131.

Rahman, M. S., Al-Belushi, R. M., Guizani, N., Al-Saidi, G. S., & Soussi, B. (2009). Fat oxidation in freeze-dried grouper during storage at different temperatures and moisture contents. *Food Chemistry, 114*(4), 1257–1264.

Rao, Q., & Labuza, T. P. (2012). Effect of moisture content on selected physicochemical properties of two commercial hen egg white powders. *Food Chemistry, 132*(1), 373–384.

Roos, Y. H. (1997). Frozen state transitions in relation to freeze drying. *Journal of Thermal Analysis and Calorimetry, 48*(3), 535–544.

Roos Y. (2009). Mapping the different states of food components using state diagrams. Modern Biopolymer Science, 261–276.

Saltmarch, M., & Labuza, T. P. (1982). Nonenzymatic browning via the Maillard reaction in foods. *Diabetes, 31*(3), 29–36.

Shah, A. K. M. A., Tokunaga, C., Ogasawara, M., Kurihara, H., & Takahashi, K. (2009). Changes in chemical and sensory properties of Migaki-Nishin (Dried Herring Fillet) during drying. *Journal of Food Science, 74*(7), S309–S314.

Tahergorabi, R., Hosseini, S.V., & Jaczynski, J. (2011). Seafood proteins. In: Philllips & Williams (eds) Handbook of food proteins, pp 116-149. Woodhead Publishing Series in Food Science, Technology and Nutrition (222), Cambridge, UK.

Torii, H., Tatsumi, T., & Tasumi, M. (1998). Effects of hydration on the structure, vibrational wavenumbers, vibrational force field and resonance raman intensities of N-methylacetamide. *Journal of Raman Spectroscopy, 29*(6), 537–546.

White, K. L., & Bell, L. N. (1999). Glucose loss and Maillard browning in solids as affected by porosity and collapse. *Journal of Food Science, 64*(6), 1010–1014.

Zamora, R., & Hidalgo, F. J. (2005). Coordinate contribution of lipid oxidation and Maillard reaction to the nonenzymatic food browning. *Critical Reviews in Food Science and Nutrition, 45*(1), 49–59.

Zhou, P., Liu, X., & Labuza, T. P. (2008). Effects of moisture-induced whey protein aggregation on protein conformation, the state of water molecules, and the microstructure and texture of high-protein-containing matrix. *Journal of Agricultural and Food Chemistry, 56*(12), 4534–4540.

Zhu, S., Luo, Y., Hong, H., Feng, L., & Shen, H. (2013). Correlation between electrical conductivity of the gutted fish body and the quality of bighead carp (*Aristichthys nobilis*) Heads Stored at 0 and 3 ° C. *Food and Bioprocess Technology, 6*, 3068–3075.